PHYSICAL REVIEW B VOLUME 50, NUMBER 9 1 SEPTEMBER 1994-I

Dynamics of irreversible island growth during submonolayer epitaxy

G.S. Bales and D.C. Chrzan
Computational Materials Science Department, Sandia National Laboratories, Livermore, California 94551-0969
(Received 4 March 1994)

The nucleation and growth of two-dimensional islands during the submonolayer stage of epitaxial growth is studied with kinetic Monte Carlo simulations and mean-field rate equations. Previous work on irreversible growth is extended to include relaxation of island shapes by edge diffusion. Island morphologies range from ramified structures at low temperatures to compact, polygonal shapes at higher temperatures. Using a self-consistent calculation of the rate coefficients, *quantitative* agreement is obtained between the solution to coupled, mean-field rate equations and the simulation results for average quantities. The island size distribution function is described by a single universal "scaling function." The average island size is the only important scale for determining island densities. It is shown that the general form of the scaling *ansatz* applies to wider range of coverages than anticipated previously. This scaling form is combined with the solution to the rate equations to explore explicitly the $\frac{D}{F}$ dependence of the number density of islands (D is the surface diffusion coefficient and F is the deposition flux).

I. INTRODUCTION

Experimental techniques for studying the nucleation and growth of epitaxial thin films have progressed rapidly over the past few years. Scanning tunneling microscopy[1] (STM) provides detailed atomic scale information. Low-energy electron microscopy[2] provides real-time images of the growing film with 100-Å resolution and a field of view spanning several micrometers. Thus, the collective dynamics of the evolving adlayer are readily studied. In addition, reciprocal-space techniques, such as low-energy electron diffraction[3] and *in situ* grazing incidence x-ray scattering,[4] provide information on long-range correlations in the growing films. The variety of experimental data for length scales ranging from angstroms to microns, and times ranging from picoseconds to minutes provide the opportunity to develop a quantitative theory of thin film growth. The "ideal" theory should span these length and time scales to connect first-principles electronic structure calculations with thin-film morphology.

Models of epitaxial growth under typical molecular-beam-epitaxy (MBE) conditions commonly assume the following: Atoms are deposited at random onto an initially flat substrate at a rate of F monolayers/sec, and diffuse freely on the crystalline substrate until they encounter another atom, group of atoms, or a defect such as a step. Immediately upon application of the flux to a defect-free area of the substrate, the population of isolated adatoms begins to increase linearly with time until small clusters (or islands) begin to nucleate. As the deposition proceeds, the total number of islands increases, eventually overtaking the number of monomers. The period of time between this crossing of the monomer and island densities, and the initial stages of coalescence is referred to as the "aggregation regime." In this regime the film growth is characterized completely by the dynamical evolution of the island size distribution, island shapes, and locations.

This work focuses on the study of the aggregation regime for systems in which the overlayer wets the substrate. The islands that form in this so-called "Frank–van der Merwe growth mode" are only one atomic layer in thickness. The observed morphology of these two-dimensional islands range from ramified structures similar to those observed in two-dimensional models of diffusion limited aggregation[5] (DLA) to compact polygonal shapes. Recent STM studies[1] of films grown at room temperature reveal ramified islands for Au on Ru (0001) and compact islands for Co on Ru (0001). Similar studies of Pt on Pt produced ramified islands at low temperature and compact islands at higher temperatures.[6] The varying morphologies reflect the complex nature of the dynamical processes in this non-equilibrium system. Local rearrangements of atomic positions within an island drive the island to a compact polygonal shape, while mass transport to the islands drives instabilities in the island morphology.[7,8]

It is important to understand the effect that the atomic-scale processes have on the island shapes and distributions, since these islands form the building blocks upon which all further growth proceeds. For example, the morphology of the first monolayer has a large influence on the nucleation and growth of the second and subsequent layers. This fact is clearly demonstrated in the work of Kunkel *et al.*, which linked the formation of ramified islands to the observation of anomalous reentrance of layer-by-layer growth of Pt on Pt at low temperature.[9]

Moreover, recent authors have proposed a direct way of calculating the surface diffusion coefficient D by simply counting the number of islands on the substrate.[10] The number of islands per unit area N has been observed to have (approximately) a simple power-law dependence[11] on the surface diffusion coefficient and the flux F according to

0163-1829/94/50(9)/6057(11)/$06.00 ©1994 The American Physical Society

$$N \propto (D/F)^{-\gamma} . \quad (1)$$

The so-called "minimal-model" proposed by Villain *et al.*[12] assumes that apart from a small logarithmic correction, average quantities, such as N, scale with a single length, namely,

$$\ell \propto (D/F)^{\gamma/2} . \quad (2)$$

This assumption is argued to be valid in the latter part of the aggregation regime in the adiabatic limit for the monomer densities. From straightforward scaling arguments and the assumption that coalesence limits the number of islands on the substrate, Villain *et al.* predicted values for γ ranging from 1/3 to 1/2. The exponent is found to depend on the types of diffusional processes assumed important for the specific material.

Much of the theoretical work from the past 25 years focuses on the solution to a set of deterministic coupled reaction-diffusion (or rate) equations[11,13] that describe the dynamical evolution of the island size distribution function $\langle n_s(\theta)\rangle$. (The island size distribution function $\langle n_s(\theta)\rangle$ is defined as the number of islands per unit area containing s atoms at a coverage $\theta = Ft$. The angular brackets represent an average over a large area of the surface or an ensemble of systems.) As input into the rate equations, one specifies rate coefficients that contain information concerning all of the important atomic scale processes as well as long-range correlations between islands. The exact specification of these rates requires the solution to a far-from-equilibrium many-body problem. The complexity of the problem requires one to make approximations. Ideally, the resulting solutions should be compared with experiment or computer simulations as a test of validity.

Kinetic Monte Carlo (KMC) simulations[14,15] provide a "true" solution to the stochastic problem, which can be compared directly with results from the rate equation analysis. Approximations for the capture rates can be tested for ideal systems in which all of the atomic processes have been accounted for. In principle, activation barriers for these processes can be calculated with *ab initio* techniques. In the present work, however, a limited subset of atomic-scale processes is considered, and their rates are treated as parameters. The chosen subset of processes produces irreversible growth of two-dimensional islands. In this paper, previous work on this model[16–18] is extended to include relaxation of the island shapes by edge diffusion. The details of the KMC simulations are presented in Sec. II.

Section III contains a rate equation analysis of irreversible growth, which is compared directly with KMC results. A solution to the coupled rate equations within a self-consistent mean-field approximation, similar to the "uniform depletion approximation" presented in Refs. 13 and 19, produces suprisingly accurate results. *Quantitative* agreement between KMC simulations and the rate equation results are obtained for average quantities (N, the average island size, etc.) with *one* (physically justified) fitting parameter, which depends only on the island morphology. Moreover, the nucleation rate calculated from this continuum description reproduces the results of a recent microscopic derivation for the adiabatic limit.[16]

An alternate and equally important approach to studying thin-film growth involves the application of scaling theories. Scaling theories have proven to be a powerful tool for understanding nonlinear driven dynamical systems,[20] nonequilibrium growth processes,[21] and percolation phenomena.[22] For large values of s, the distribution function $\langle n_s(\theta)\rangle$ and related quantities are determined completely by specifying the average island size $\bar{s}$ (a rigorous definition of $\bar{s}$ is presented in Sec. IV), the coverage, and a single "universal" scaling function, which is independent of coverage and the growth parameters[17]

$$\langle n_s(\theta)\rangle = \frac{\theta}{\bar{s}^2}\tilde{g}\left(\frac{s}{\bar{s}}\right) . \quad (3)$$

The coverage-dependent average island size, therefore, replaces ℓ [Eq. (2)] as the defining length (or, in this case, area). Recent *approximate* models[23,24] for growth find that $\bar{s}$ has a power-law dependence on coverage over much of the aggregation regime. More exact models[17,18,25] show that such a power-law dependence is only true approximately in the "large coverage" limit. Measuring lengths in units of ℓ and inserting the power law, $\bar{s} \sim (D/F)^{\gamma}\theta^{\beta}$, into Eq. (3), the scaling form of Ref. 23 is reproduced as

$$\langle n_s(\theta)\rangle = \theta^{1-2\beta}(D/F)^{-2\gamma}\tilde{g}\left[s\,\theta^{-\beta}(D/F)^{-\gamma}\right] . \quad (4)$$

Equation (4) applies to coverages between approximately 0.1 monolayer and the coverage at which coalescence begins.

Section IV presents a scaling analysis of the island size distribution function. It is shown that the more general scaling form given by Eq. (3) is valid throughout the aggregation regime over a large range of coverages and ratios $\frac{D}{F}$, when one does not assume a power law for the average island size. The scaling analysis, when coupled with the mean-field solution to the rate equations provides a powerful technique for analyzing the scaling of important quantities with $\frac{D}{F}$. In particular, the scaling form is utilized to derive explicitly that the average capture rate for compact islands is independent of $\frac{D}{F}$, which facilitates the calculation of the exponent γ. For ramified islands, however, it is found that corrections to Eq. (1) arise because the average capture rate is no longer independent of $\frac{D}{F}$. This result is contrasted with the explanation of Villain *et al.*[12] Finally, Sec. V presents discussion and conclusions.

II. KINETIC MONTE CARLO SIMULATIONS

In order to study the growth of islands on a substrate under typical MBE conditions, it is necessary to consider systems that are large on the atomic scale. At low growth rates ($\sim$ 1 monolayer/min), islands on the substrate can contain over 10^4 atoms,[1] and the completion of the overlayer can take several minutes. It is not possible presently to follow the detailed trajectory of this large

number of atoms over relevant time scales using molecular dynamics. Instead, it is useful to consider a "simple" system in which atoms reside on a lattice dictated by the underlying substrate. Further simplification results from the solid-on-solid restriction in which no overhangs are allowed. The dynamics are defined by specifying transition rates for the "hopping" of atoms between adjacent lattice sites. Such simplifications allow one to model epitaxial growth on realistic length and time scales.

In contrast to standard Monte Carlo techniques, KMC is meant to reflect the time evolution of the system. This implies that one considers not only the energies of the initial and final states, but also the energy (and entropy) of the intermediate states.[14,15,26] In the following, an Arrhenius form is assumed for the "hopping rates" between adjacent sites

$$h = \nu \exp[-\beta E_B], \tag{5}$$

where ν is the attempt frequency, β is the inverse temperature, and E_B is the energy barrier separating the initial and final states. Numerical values for these parameters are difficult to calculate or measure directly and are not known in general. However, one expects E_B to depend on an atom's local environment. A very common assumption[25,27] is that the barrier for motion in *any* direction along the surface is proportional to the current number of nearest-neighbor bonds, while noting the difference between adatom-substrate bonds and adatom-adatom bonds. Hence,

$$E_B = nE + E_D, \tag{6}$$

where E_D is a constant reflecting the energy barrier for diffusion of an isolated adatom, E is a parameter reflecting the relative binding energy of an atom bound to a near neighbor (also on the surface) versus one that is not, and n is the number of lateral nearest neighbors. In the absence of an external flux, this assumption correctly drives the system to its lowest free-energy configuration.

Alternatively, a directional dependence can be incorporated into the transition rates. There is sufficient evidence to support the existence of large anisotropies in these rates, i.e., energetic barriers are known to depend on the hopping direction. The motion down a step edge, for example, is less favorable than motion on the terrace. This step edge barrier has been shown[28] to be a crucial addition in KMC calculations of the reentrance of layer-by-layer growth for Pt on Pt.[9] Also, recent embedded atom method calculations for Cu estimate that the activation barrier for detachment of an atom *from* an island is four times higher than the barrier for diffusion *along* an island edge[29] (henceforth referred to as edge diffusion). Further proof of the directional dependence for diffusion barriers is provided by the experiments performed by Hwang *et al.* on Au on Ru(0001).[1] They find that even after anealing to 650 K, no Ostwald ripening[30] of the islands is seen. However, the island shapes relax toward their compact equilibrium form due to a significant amount of edge diffusion along the boundary of the island.

With this evidence in mind, the current KMC studies assume irreversible attachment of adatoms to islands and subsequent diffusion of the adatoms along the edge of the island and/or terrace. This approximation avoids the complicating effects, which arise in the rate equation analysis due to a larger (> 1) critical nucleus. The effects of adatom surface diffusion and island structure on the size distribution function can be isolated and studied separately. The rules governing the KMC evolution of the surface are as follows.

(1) Atoms are deposited randomly onto the substrate at a rate F (monolayers/sec). All impinging atoms are assumed to stick and no desorption is allowed.

(2) Adatoms on an open terrace "hop" at a rate

$$h_D = \nu \exp[-\beta E_D]. \tag{7}$$

(Note that the diffusion coefficient is given by $D = h_D/4$ in units, where the lattice constant is one.)

(3) Attachment of monomers to the islands is irreversible. Dimers are stable and will only diffuse as the atoms move around one another.

(4) The barrier to diffusion *along the edge* of an island has a contribution of E_D from the layer below and a contribution of nE due to bonding with atoms on the same layer, where n is the number of lateral nearest neighbors. Hopping along the edge of an island, therefore, occurs at a rate given by

$$h_e = \nu \exp[-\beta(E_D + nE)]. \tag{8}$$

As mentioned earler, E_D and E are not known in general. These barriers are treated as model parameters in this paper.

(5) No additional barrier is assumed for the interlayer, downward hopping of atoms over the edge of the island. However, atoms are not allowed to hop up a layer.

Simulations are performed on a (100) surface of a simple-cubic lattice. The main results of this paper are insensitive to the underlying symmetry as long as the diffusion of free adatoms on the terrace remains isotropic. The effect of anisotropic diffusion was considered by Bartelt and Evans in an approximate model for growth.[23]

Two essential features are included in this simple model: (i) the dependence of the overall length scale on $\frac{D}{F}$, and (ii) the dependence of the island morphology on the competition between the destabilizing influence of the diffusion field[7,8] and edge diffusion. Figure 1 shows a top view of the growth of islands produced by the KMC simulations on a 400×400 lattice. Simulations for three different temperatures at the same coverage (0.4 monolayers) and growth rate are shown. The shades of gray depict the atoms on the first layer of the deposit at different stages of the growth. The lighter shades represent atoms deposited at early times while the darker shades represent those deposited at later times. The simple model is seen to produce the range of possible island morphologies found in experiment.[1,6] At low temperature [Fig. 1(a)] when the amount of edge diffusion is small, the islands are ramified and resemble the fractal structures produced in two-dimensional DLA models.[5] Since an island grows

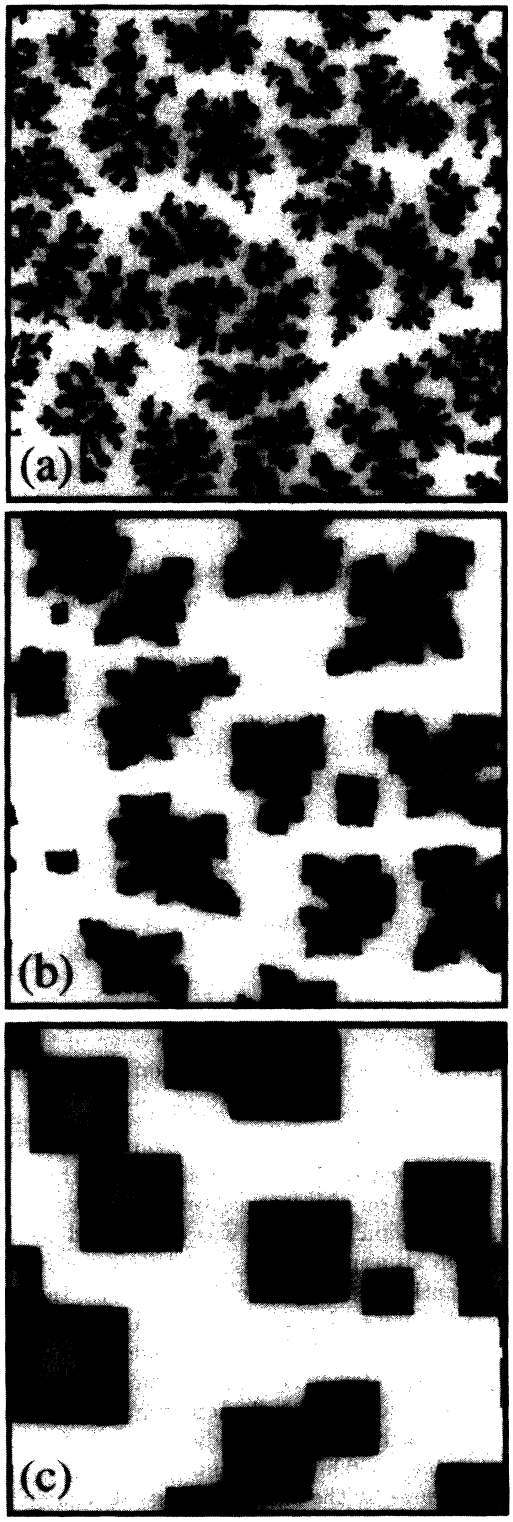

FIG. 1. Kinetic Monte Carlo simulations of irreversible island growth at three different temperatures: (a) $T = E_D/16$, $\frac{D}{F} \simeq 1 \times 10^{10}$; (b) $T = E_D/14$, $\frac{D}{F} \simeq 8 \times 10^{10}$; and (c) $T = E_D/10$, $\frac{D}{F} \simeq 4 \times 10^{12}$. The barrier to edge diffusion $E = E_D$. The lighter shades of gray represent atoms deposited at early times, while the darker shades represent those deposited at later times.

in the direction from which the adatoms are diffusing, there is a tendency for the islands to avoid one another. This tendency delays coalescence and increases the range of the aggregation regime. Atoms that fall on top of the islands are quickly incorporated into the inner portions of the island.

At a slighty higher temperature [Fig. 1(b)], edge diffusion begins to play an important role. The branches are wider and the shapes resemble the growth of dendrites. The islands are still able to avoid one other, and the coverage at which coalescence begins is comparable to the lower-temperature case.

At a much higher temperature [Fig. 1(c)], edge diffusion is very rapid. The shape of the islands relax to their equilibrium form; a square on the (100) surface. Since the shape of the island is restricted to a square, they can no longer avoid one another. Coalescence is observed already at 0.4 monolayers. In addition, there are fewer islands than the low-temperature case because the surface diffusion rate has increased [consistent with Eq. (1)]. Quantitative results from the KMC simulations are presented in the next two sections.

III. RATE EQUATION ANALYSIS

Rate equations provide a useful tool for understanding the early stages of epitaxial growth. In this section, coupled rate equations, which describe the time evolution of the island size distribution function $\langle n_s(\theta)\rangle$, are derived. In what follows, only those terms in the rate equations appropriate for the simplified set of processes described in the preceding section are retained. The evolution of the island size distribution function is followed from early times up until the islands start to coalesce. Under these assumptions the coverage derivative (time is replaced by the coverage $\theta = Ft$) of $\langle n_s(\theta)\rangle$ is given by

$$\frac{d\langle n_s\rangle}{d\theta} = (D/F)\,\sigma_{s-1}\langle n_1\rangle\langle n_{s-1}\rangle - (D/F)\,\sigma_s\langle n_1\rangle\langle n_s\rangle + \kappa_{s-1}\langle n_{s-1}\rangle - \kappa_s\langle n_s\rangle \qquad \{s = 2,\ldots,\infty\} \tag{9}$$

where D is the adatom diffusion constant. The capture number, σ_s, is a measure of how effectively an island of size s competes for the available monomers on the surface. The first (second) term on the right-hand side of this equation is the rate at which diffusing monomers are added to an island of size $s-1(s)$ multiplied by the total density of islands of that size. This process increases (decreases) the number of islands of size s. The third and fourth terms account for the direct capture of deposited atoms by an island of size $s-1$ and s respectively. In the quasistatic approximation (see below) $\kappa_s \simeq s^{2/d_f}$ with d_f the fractal dimension of the islands. At large values of $\frac{D}{F}$ and small coverages these direct capture terms are small and do not effect the exponent in Eq. (1).

The density of monomers is described by

$$\frac{d\langle n_1\rangle}{d\theta} = 1 - 2\,(D/F)\,\sigma_1\langle n_1\rangle^2 - (D/F)\,\langle n_1\rangle \sum_{s=2}^{\infty} \sigma_s\langle n_s\rangle - \kappa_1\langle n_1\rangle - \sum_{s=1}^{\infty} \kappa_s\langle n_s\rangle \tag{10}$$

where the first term on the right-hand side results from the flux of atoms onto the surface. The second and third terms account for the loss of monomers to dimer formation and attachment to islands, respectively. The factor of 2 in the second term is present because each dimer formation results in the loss of two monomers. The fourth term accounts for the loss of diffusing monomers due to direct capture of the deposited flux, and the fifth term is the loss of flux to the direct impingement onto existing islands and monomers.

Note that all information about island structure and the spatial correlations between islands is contained in the time-dependent capture numbers σ_s. Complete information about the correlations is not contained in the average quantities $\langle n_s(\theta)\rangle$. The system of equations given by Eqs. (9) and (10), therefore, are not complete without further information or assumptions. In this section, approximations are presented in which the capture numbers can be specified completely, given knowledge of the average densities, i.e., $\sigma_s = \sigma_s(\langle n_1\rangle, \langle n_2\rangle, \ldots)$. Numerous approximations of this form exist in the literature. References 11 and 13 provide excellent reviews. In this work, mean-field assumptions similar in spirit to the "uniform depletion" approximation[13,19] are employed. Analogous techniques have been used for the study of radiation damage in solids[31] and Ostwald ripening.[32]

Consider an island of radius R_s (assumed to be circular) embedded in an ensemble average system of islands and monomers. The local density of monomers, $n_1(\mathbf{r},\theta)$, responds to the presence of this island. In particular, if adatoms attach irreversibly, the density of monomers vanishes at the edge of the island: $n_1(R_s,\theta) = 0$. The simplest possible diffusion equation,[33] which describes the spatial variations of n_1 is

$$\frac{\partial n_1}{\partial \theta} = (D/F)\,\nabla^2 n_1 + \mathcal{J} - (D/F)\,\xi^{-2} n_1, \tag{11}$$

where $\mathcal{J}$ and ξ can be calculated from the self-consistency condition, $n_1(\mathbf{r}\to\infty,\theta) = \langle n_1(\theta)\rangle$, i.e., the presence of this island is not felt infinitely far away. In this limit, Eq. (11) must reproduce Eq. (10). Direct comparison gives

$$\mathcal{J} = 1 - \sum_{s=1}^{\infty} \kappa_s\langle n_s\rangle \tag{12}$$

and

$$\xi^{-2} = 2\sigma_1\langle n_1\rangle + \sum_{s=2}^{\infty} \sigma_s\langle n_s\rangle + (F/D)\,\kappa_1, \tag{13}$$

where ξ is the average distance a monomer travels before being captured by an island or another monomer and $\mathcal{J}$ is the fraction of the flux, which lands on the bare substrate. Implicit in this approach is the *mean-field* assumption that at every point outside of the island, the local densities $n_s(\mathbf{r},\theta)$ take on their average value $\langle n_s(\theta)\rangle$ (for $s \geq 2$).

Despite its deceptively simple form, Eq. (11) is difficult to solve due to its complicated time dependence [$\xi = \xi(t)$] and the growth of the island, i.e., the boundary is moving. An approximate solution can be found, however, by assuming that the rate of adatom diffusion is large compared to the growth rate of the island (a good approximation). It is sufficient, then, to fix the radius of the island and solve for the instantaneous concentration of monomers. One must be careful to assure that the boundary condition at large $\mathbf{r}$ is satisfied; hence, it is *not* appropriate to simply neglect the left-hand side of Eq. (11). One cannot satisfy Eq. (10) as $r \to \infty$ if the coverage (time) derivative of the more general $n(r,\theta)$ is neglected. Instead, substract Eq. (10) from Eq. (11) and neglect deviations of the coverage derivative from its average value:

$$\frac{F}{D}\left(\frac{\partial n_1}{\partial\theta} - \frac{d\langle n_1\rangle}{d\theta}\right) = \nabla^2 n_1 - \xi^{-2}(n_1 - \langle n_1\rangle) \approx 0. \tag{14}$$

The resulting Helmholtz equation has the straightforward solution

$$n_1(r,\theta) = \langle n_1\rangle\left[1 - \frac{K_0\,(r/\xi)}{K_0\,(R_s/\xi)}\right] \tag{15}$$

with K_j a modified bessel function of order j. From this, one can readily obtain the capture numbers,[11]

$$\sigma_s = \frac{2\pi R_s}{\langle n_1\rangle}\left.\frac{\partial n_1}{\partial r}\right|_{r=R_s} = 2\pi\frac{R_s}{\xi}\frac{K_1\,(R_s/\xi)}{K_0\,(R_s/\xi)}. \tag{16}$$

Since the capture numbers can be written as functions of the average densities, Eqs. (9), (10), (13), and (16) form a complete set of equations that must be solved self-consistently for the island size distribution function. Calculation of σ_s with Eq. (16) is accomplished easily using an iterative scheme. The resulting set of ordinary differential equations are solved numerically with a standard integration routine (it is only necessary to consider values of s up to a maximum value, which is greater than the size of the largest island). However, two outstanding issues remain: (1) The islands seen in Fig. 1 are *not* circular, and (2) one does not expect this continuum approach to apply to small values of s (especially the mobile monomers, $s = 1$).

For noncircular islands, it is sufficient to replace the radius R_s with an effective radius appropriate to the island morphology. At low temperatures (or no edge diffusion) when the islands are ramified, the effective radius has a power-law dependence on s given by

$$R_s \simeq \alpha s^{1/d_f}, \tag{17}$$

where d_f is the fractal dimension of the islands[16] measured to be $d_f \approx 1.72$. Since the inner portions of the fractal islands fill in due to deposition, α is a weakly time-dependent quantity, which is taken to be nearly constant ($\alpha \simeq 1.0$). Note that α is the only fitting pa-

rameter in the theory that depends only on the island structure. For compact islands at higher temperatures (large amount of edge diffusion), the distinction between square and circular islands produces minor differences in the solutions to the rate equations. For circular islands the radius is given by

$$R_s \simeq \sqrt{\frac{s}{\pi}}, \tag{18}$$

i.e., $d_f = 2$ and $\alpha = 1/\sqrt{\pi}$. For square islands, however, a better result is obtained with a larger value for α ($\alpha \simeq 0.95$). For intermediate temperatures, the islands remain compact until a critical size is reached. Subsequent growth produces ramified islands with R_s of the from given by Eq. (17). This work focuses on the two extreme limits (compact or fractal), while noting the need for further analysis. An estimate of the critical size, for example, can be obtained from a linear stability analysis of Eq. (11).[7,8]

The continuum approach produces an excellent estimate for σ_s even for the smaller values of s. Far away from the island and/or monomer, one expects Eq. (15) to remain robust. The results indicate that the solution is not very sensitive to near-field corrections due to the small size or shape of the island. The use of Eq. (16) down to values of $s = 1$ produces excellent results (see below). One must be careful, however. From the perspective of a monomer, the other monomers are diffusing at a rate $D' = 2D$. One then solves for σ_1 using the method above with D replaced by D'. To avoid double counting, the derived capture number, must be divided by two. This cancels the correction on the diffusion constant and produces the same results as Eq. (16). In fact, this capture number reproduces the result of a recent microscopic derivation of the dimer formation rate in the adiabatic approximation.[16] This approximation is good at larger coverage and assumes that $d\langle n_1\rangle/d\theta \simeq 0$ and $N \gg \langle n_1\rangle$. Furthermore, since $\xi \gg R_1$, Eq. (16) can be replaced by its small argument expansion. After combining Eqs. (10) and (16), one obtains,

$$\sigma_1 \simeq \frac{4\pi}{\ln\left[(1/\alpha)\,(D/F)\,\langle n_1\rangle\right]}. \tag{19}$$

In Fig. 2, a numerical solution of the rate equations is compared with results from KMC simulations for the case of no edge diffusion (the barrier to edge diffusion is set to a very large number). Plots of the monomer density,[35] $\langle n_1\rangle$, and total number density of islands N versus coverage are shown for three different values of $\frac{D}{F}$; (a) 10^5, (b) 10^7, and (c) 10^9. The coverage ranges from 0.0 to 0.4 monolayers. The dashed lines are solutions to the rate equations and the solid lines are KMC results. The agreement between the mean-field rate equations and the KMC simulations is striking. Similar agreement is obtained for conditions yielding compact islands.

Figure 3 shows a plot of the second moment of the size distribution $\bar{s}(\theta)$ (defined in the next section) for the same values of $\frac{D}{F}$. The agreement between the rate

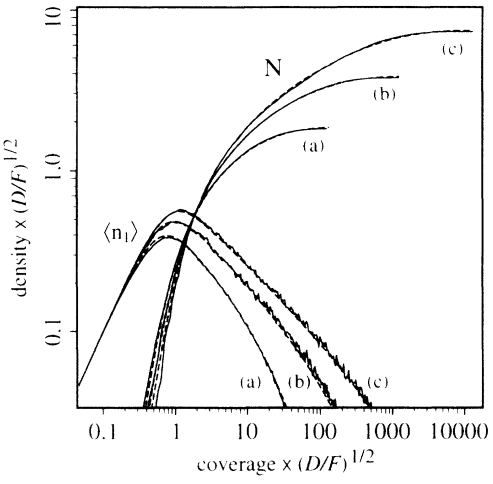

FIG. 2. Monomer density $\langle n_1(\theta)\rangle$ and total number density of islands $N(\theta)$ versus coverage for ramified islands at (a) $\frac{D}{F} = 10^5$, (b) $\frac{D}{F} = 10^7$, and (c) $\frac{D}{F} = 10^9$. The solid lines are measured from KMC simulations, and the dashed lines are numerical solutions of the rate equations.

equations and the KMC simulations is also very good. At larger coverages, however, the island size distribution function $\langle n_s(\theta)\rangle$ is not reproduced very well by the mean-field rate equations. Figure 4 shows the distribution at three different coverages for $\frac{D}{F} = 10^8$. Hence, the rate equations are seen to reproduce average quantities but *not* the distribution function. This is not surprising, since the mean-field approximation does not properly include island-island correlations. The following section discusses the scaling properties of this distribution.

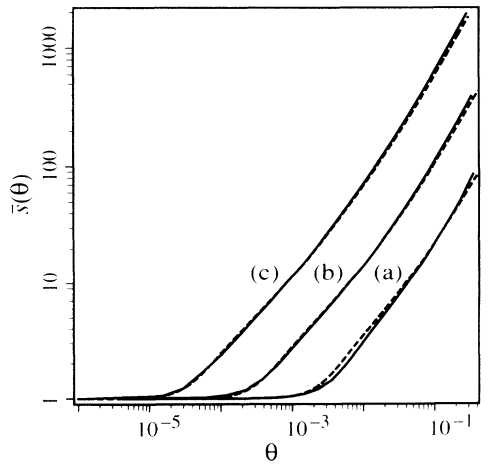

FIG. 3. Average island size $\bar{s}$ versus coverage for ramified islands at (a) $\frac{D}{F} = 10^5$, (b) $\frac{D}{F} = 10^7$, and (c) $\frac{D}{F} = 10^9$. The solid lines are measured from KMC simulations, and the dashed lines are numerical solutions of the rate equations.

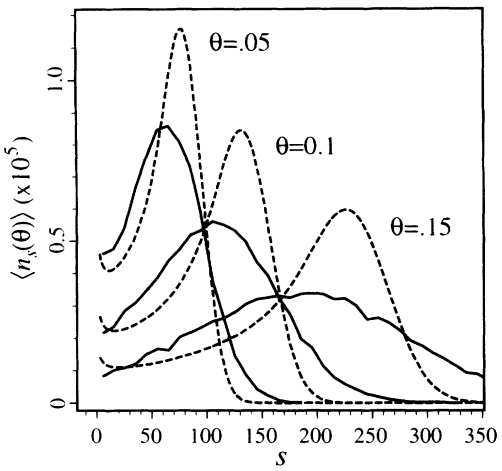

FIG. 4. Island size distribution $\langle n_s(\theta)\rangle$ versus s at three different coverages. The solid lines are measured from KMC simulations, and the dashed lines are numerical solutions of the rate equations.

IV. SCALING THEORY

The distribution function, defined by

$$p(s,\theta) = \frac{s\langle n_s(\theta)\rangle}{\sum_{s=1}^{\infty} s\langle n_s(\theta)\rangle} = \frac{s\langle n_s(\theta)\rangle}{\theta}, \tag{20}$$

is equal to the probability that an atom, selected at random from the growing layer, resides in an island that contains s atoms. This section focuses on the dependence of this distribution on the coverage and growth parameters and the consequences of such dependencies.

The average size island $\bar{s}(\theta)$, to which an atom belongs at a coverage θ, is given by the first moment of Eq. (20) according to

$$\bar{s}(\theta) = \sum_{s=1}^{\infty} sp(s,\theta) = \frac{\sum_{s=1}^{\infty} s^2\langle n_s(\theta)\rangle}{\theta}. \tag{21}$$

An alternate average island size can be defined by

$$s_{\mathrm{av}}(\theta) = \frac{\sum_{s=1}^{\infty} s\langle n_s(\theta)\rangle}{\sum_{s=1}^{\infty}\langle n_s(\theta)\rangle} = \frac{\theta}{N + \langle n_1\rangle}. \tag{22}$$

In this paper, a bar over a symbol denotes an average over the distribution given by Eq. (20), while the subscript av denotes an average over the distribution $\langle n_s(\theta)\rangle/(N + \langle n_1\rangle)$ as in Eq. (22).

After the initial transient period, when the number of islands becomes much greater than the number of monomers, the finite size of the atom no longer influences the behavior of the distribution function. The only important size scale for determining the distribution function becomes the average size of an island (since units are chosen so that an atom occupies unit area, an island containing s atoms has an area of s). Furthermore, the distribution function only depends on the coverage through this characteristic size, i.e., $p(s,\theta)$ is a homogeneous function of s and $\bar{s}(\theta)$. Given the requirement of mass conservation and normalization, the scaling hypothesis implies that the distribution function must have the form[21,22]

$$p(s,\theta) = \bar{s}^{-1} g\left(\frac{s}{\bar{s}}\right), \tag{23}$$

where $g(z)$ is a universal function, which is independent of $\frac{D}{F}$ and satisfies $\int_0^\infty dz\, g(z) = \int_0^\infty dz\, zg(z) = 1$. The scaling function, $g(z)$, is related to $\tilde{g}(z)$ in Eq. (3) by $g(z) = z\tilde{g}(z)$. Futhermore, one can show that

$$\bar{s} = \frac{\zeta\theta}{N + \langle n_1\rangle} \simeq \frac{\zeta\theta}{N}, \tag{24}$$

where $\zeta = \int dz\, g(z)/z$, a constant. Scaling is only expected to hold when $N \gg \langle n_1\rangle$; hence, the $\langle n_1\rangle$ in the denominator of Eq. (22) can be neglected.

This scaling ansatz predicts that a plot of $\bar{s}p(s,\theta)$ as a function of $s/\bar{s}$ should produce a curve, $g(z)$, independent of the coverage and $\frac{D}{F}$ (in the aggregation regime). Figure 5 presents a test of this prediction using KMC results. In panel (a), the data for several different coverages at one value of the ratio $\frac{D}{F} = 10^8$ are plotted as suggested above for the case of fractal islands (no edge relaxation). For coverages ranging from less than 0.001 to more than 0.4, the data collapse is excellent. The resulting curve is the scaling function. Panel (b) shows the scaling function for a single coverage (0.2 monolayers) for three different values of $\frac{D}{F}$. Again, excellent data collapse is observed. The last curve in panel (b) (represented by a ◇) is the result for the case of compact islands. The scaling is insensitive to the growth parameters and the structure of the islands. The fact that the results for several different conditions result in a unique curve is proof of the applicability of the scaling form.

Given the observation of scaling behavior for the probability function $p(s,\theta)$, it is worthwhile to pursue further scaling properties of the system. In particular, the applicability of Eq. (1) to these simulations can be explored and the exponent γ can be deduced from the form of the differential equations[36] with the aid of Eq. (23). Since $\bar{s}$ is setting the size scale, it is important to calculate the dependence of $\bar{s}$ on the growth parameters. According to Eq. (23), the effect of varying these growth parameters on the island densities is contained in $\bar{s}$. An equation for $\bar{s}$ is obtained by substituting Eqs. (9) and (10) into the coverage derivative of Eq. (21). Neglecting direct attachment, $\bar{s}$ obeys

$$\frac{d}{d\theta}\left[\theta\,(\bar{s} - 1)\right] = 2\,(D/F)\,\langle n_1\rangle\bar{\sigma}\theta. \tag{25}$$

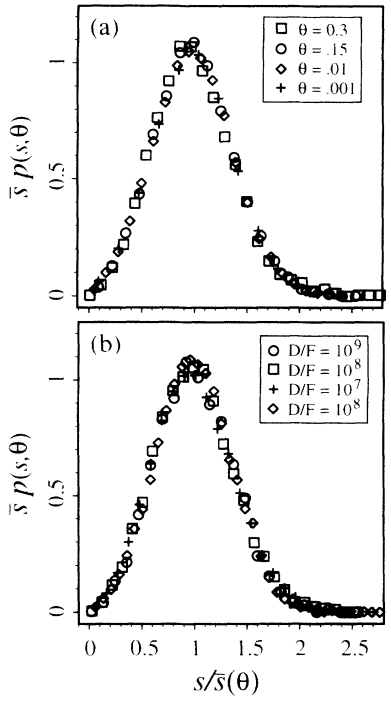

FIG. 5. Scaling function for varying growth conditions and coverage. Panel (a) is for fixed $\frac{D}{F} = 10^8$ at four different coverages for ramified islands. Panel (b) shows the scaling functions at fixed coverage ($\theta = 0.2$) for ($\bigcirc$, $\square$, and $+$) three different values of $\frac{D}{F}$ for ramified islands, and ($\diamond$) $\frac{D}{F} = 10^8$ for compact square islands.

Summing Eq. (9) and neglecting $\langle n_1 \rangle$ with respect to N in Eq. (10) gives

$$\frac{dN}{d\theta} = (D/F)\,\sigma_1 \langle n_1 \rangle^2 \tag{26}$$

and

$$\frac{d\langle n_1 \rangle}{d\theta} = 1 - (D/F)\,\langle n_1 \rangle \sigma_{\rm av} N. \tag{27}$$

The $\frac{D}{F}$ dependence of N, $\langle n_1 \rangle$, and $\bar{s}$ can be derived from Eqs. (25)–(27) only if the effect of these growth parameters on $\sigma_{\rm av}$ and $\bar{\sigma}$ is known. This is facilitated by the scaling ansatz if one assumes the rate coefficients to take the simple form (as in the mean-field calculations), $\sigma_s = \sigma(s\xi^{-d_f})$. Then, $\sigma_{\rm av}$ is given by

$$\begin{aligned} \sigma_{\rm av} &= \frac{1}{N} \sum_{s=1}^{\infty} \sigma_s \langle n_s(\theta) \rangle \\ &\simeq \frac{1}{\zeta} \int_{z \simeq 0}^{\infty} \frac{dz}{z} \sigma \left(\frac{\bar{s} z}{\xi^{d_f}} \right) g(z) \\ &= f\left(\bar{s} \xi^{-d_f} \right). \end{aligned} \tag{28}$$

From the definition of ξ [Eq. (13)], for $N \gg \langle n_1 \rangle$,

$$\bar{s}\xi^{-d_f} = \bar{s}^{(1-d_f/2)} \left[\zeta \theta f\left(\bar{s}\xi^{-d_f} \right) \right]^{d_f/2}. \tag{29}$$

Assuming that Eq. (29) can be solved for $\bar{s}\xi^{-d_f}$, the resulting value of $\bar{s}\xi^{-d_f}$ is a function only of $\theta \bar{s}^{(2/d_f - 1)}$. Therefore, $\sigma_{\rm av}$ must have the form

$$\sigma_{\rm av} = \tilde{f}\left(\theta \bar{s}^{(2/d_f - 1)} \right). \tag{30}$$

All of the dependence on $\frac{D}{F}$ in this equation is contained in the average size $\bar{s}$. In particular, for compact islands, $d_f = 2$ and $\sigma_{\rm av}$ is found to be *independent of* $\frac{D}{F}$. A similar analysis can be performed for $\bar{\sigma}$, i.e., $\bar{\sigma} = \bar{\sigma}\left(\theta \bar{s}^{(2/d_f - 1)} \right)$. Note that the above result applies *only* in the scaling regime.

At larger coverage in the adiabatic limit for the monomer density, the left-hand side of Eq. (27) is small in comparison to the right-hand side. If one neglects the weak logarithmic dependence of σ_1 on $\frac{D}{F}$, it is easy to show from Eqs. (25)–(27) that

$$\begin{aligned} N(\theta) &\sim (D/F)^{-\gamma}, \\ \langle n_1(\theta) \rangle &\sim (D/F)^{-(\gamma+1)/2}, \\ (\bar{s}(\theta) - 1) &\sim (D/F)^{\gamma} \end{aligned} \tag{31}$$

with the exponent, $\gamma = 1/3$ for compact islands. These results have been derived previously[11,12,16,17,23] for the irreversible model by *assuming* that $\sigma_{\rm av}$ is independent of D/F. The current analysis provides a justification for this assumption for the case of compact islands.

For fractal islands, however, $\sigma_{\rm av}$ is no longer independent of $\frac{D}{F}$. Equations (25)–(27) have a parametric form, and it is not possible to extract analytically a simple power-law with coverage-independent exponents. Corrections to Eq. (31), however, are small and time dependent. Figure 6 shows scaled plots of N, $\langle n_1 \rangle$, and $(\bar{s} - 1)$ versus coverage for values of $\frac{D}{F}$ ranging from 10^5 to 10^{10} for *ramified* islands. At early coverages ($\theta \lesssim 0.1$), exponents for the compact island case provide a good description of the data for the monomers and average islands size (see below). At larger coverages the difference between compact and fractal islands is more pronounced and *small* deviations from Eq. (31) are observed. In Fig. 7 the total island density is plotted versus $\frac{D}{F}$ at a fixed coverage ($\theta = 0.2$). The slope of the *curve* for the fractal island case is larger than for the compact island case. Again, the rate equations provide the correct value for these number densities.

Villain *et al.*[12] proposed a correction for the value of γ for fractal islands based on the assumption that *only coalescence* can limit the total number of islands. The effect of coalescence, however, is *not* included in the self-consistent rate equations. The dependence of N on D/F is altered from the compact island case long before coalescence can play a role. Therefore, a different physical interpretation emerges. The difference in size of a fractal versus compact island increases with the average island size and, hence, with $\frac{D}{F}$. The larger ramified islands compete more effectively for the available monomers, leaving fewer monomers for island nucleation. The net result is a decrease in the total number of islands when compared

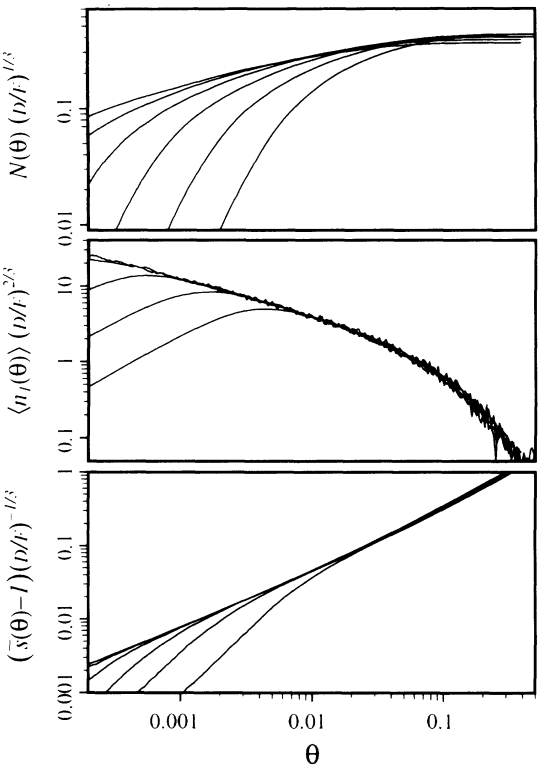

FIG. 6. Scaled plots of $N(\theta)$, $\langle n_1(\theta)\rangle$, and $(\bar{s}(\theta)-1)$ versus coverage for ramified islands. Each panel shows five different values for $\frac{D}{F}$ ranging from 10^5 to 10^{10}. $\frac{D}{F}=10^5$ is the first to diverge from the universal curve as the coverage decreases.

with the compact-islands case.

The deviation of the curves in Fig. (6) from the universal curve at lower coverage occurs when the system has not yet reached the adiabatic limit. This seems to occur at a higher coverage for N than for the other quantities of interest. In fact, $\langle n_1\rangle$ and $(\bar{s}-1)$ scale throughout the aggregation regime. This is fully consistent with Eq. (24). Assuming the scaling form to be correct for $(\bar{s}-1)$, N must have the form $N \sim \theta/[1+\left(\frac{D}{F}\right)^{(\gamma)} q(\theta)]$, where $q(\theta)$ is the function shown in Fig. 6(c). Until $\bar{s}$ becomes much greater than one, both N and $\bar{s}-1$ cannot obey Eq. (31). The coverage at which this occurs goes to zero as $\left(\frac{D}{F}\right)\to\infty$.

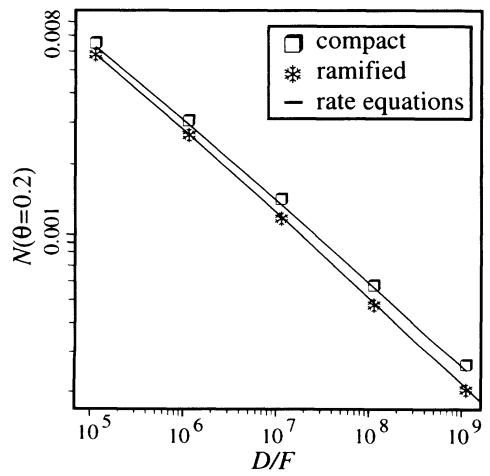

FIG. 7. Number density of islands N versus $\frac{D}{F}$ at a fixed coverage ($\theta=0.2$) for compact ($d_f=2$, $\alpha=0.95$) and fractal ($d_f=1.72$, $\alpha=1.0$) islands.

Using an analysis similar to that which resulted in Eq. (30), the exponents in Eq. (31) predicted by other approximations for σ_s can easily be derived. For example, it is common to assume that the capture number is proportional to the perimeter of the island,[18,24,37] i.e., $\sigma_s = as^p$. Missing from this approximation is the influence of the other islands. Based on this assumed form for σ_s, from Eq. (23) one can show that $\sigma_{\rm av} \sim \bar{s}^p$, which, when inserted into Eqs. (25)–(27), produces an *incorrect* estimate for γ, viz., $\gamma = 1/(2p+3)$. Ratsch *et al.*[25] recognized this problem and proposed capture numbers of the form $\sigma_s = aN^q s^p$. The current analysis reveals that, for *compact* islands, the correct γ is obtained if the capture number is any integrable function of $(Ns)^p$ $(p=q)$. The classical derivations[11,13] for the rate coefficients presented as functions of R_s/ℓ, where $\ell = 1/\sqrt{\pi N}$ is the average distance between islands, satisfy this criteria, since $R_s/\ell \sim \sqrt{Ns}$ (compact islands). Such derivations provide better physical insight than simple fitting to power laws. In particular, the self-consistent, mean-field description produces results which are superior to that produced by oversimplified, power-law approximations for the capture rates.

V. CONCLUSION

This paper presents a detailed analysis of the growth of two-dimensional islands during the early stages of epitaxy. Direct comparison between numerical solutions to the rate equations and KMC simulations produces surprising results. A straightforward, self-consistent, mean-field treatment of the rate equations produces quantitative agreement for average quantities. The theoretical framework for calculating the rate coefficients was discussed over 20 years ago in a review article by Venables.[13] Direct comparison with KMC simulations have allowed a refinement of these techniques. In particular, we have extended the formalism of Venables to apply to ramified and noncircular islands with the introduction of the island dimensionality d_f and one fitting parameter.

Despite the quality of such approximations, much of the recent theoretical work has focused on a crude power-law form for the rate coefficients, namely, $\sigma_s = s^p$. Such simplifications provide the correct qualitative behavior and aid in the derivation of analytic results. It can only produce quantitative accuracy, however, if desorption from the surface is allowed to "short circuit" the communication between islands. If the desorption rate is small, the results can be misleading. The dependence of the number of islands on $\frac{D}{F}$, for example, is not correctly reproduced for the irreversible model. Furthermore, the average island size is predicted to have a power-

law dependence on coverage for much of the aggregation regime.[24] No such power law is observed in the KMC simulations or the mean-field analysis presented in this work.

This has particular significance in the final form of the scaling ansatz [Eq. (23)]. If $\bar{s}$ is assumed to have a power-law dependence on θ the scaling ansatz takes the form of Eq. (4). Equation (4) was first proposed by Bartelt and Evans[23] to describe the scaling behavior for the growth of point islands. In their model, each island occupies only one point on the substrate and the exponents γ and β are found to be 1/3 and 2/3, respectively. For islands of finite extent, however, the nucleation rate must saturate at higher coverage as the amount of room left for new nucleation decreases. In this case, N approaches a constant and $\beta = 1$ (Refs. 18 and 25) [see Eq. (24)]. The point island exponent ($\beta = 2/3$) is *never* observed in the KMC simulations presented in this work, and the asymptotic approach of $\bar{s}$ to a linear form is valid approximately only over a limited range. Instead, it is shown here that the entire aggregation regime obeys the more general scaling form given by Eqs. (3) or (23) when $\bar{s}$ is *not* restricted to a power law.

An important conclusion derived from the scaling ansatz is that the mean-field, average capture number σ_{av} for *compact* islands is independent of $\frac{D}{F}$ in the scaling regime. This leads directly to the correct power-law dependence of N and $\langle n_1 \rangle$ on $\frac{D}{F}$ thus justifying derivations presented in previous studies of irreversible growth.[12,16,23] Furthermore, the mean-field analysis reveals that deviations from this simple dependence for the case of fractal islands are due primarily to the nontrivial dependence of σ_{av} on $\frac{D}{F}$ when $d_f \neq 2$.

The details of the island size distribution are not reproduced by the mean-field analysis (or the simpler approximations discussed at the end of Sec. IV). In particular, the scaling form predicted by Eq. (23) or, equivalently, Eq. (3) is *not* an exact solution of the rate equations. Further analysis of the distribution function requires a detailed analysis of the island-island correlations and how these correlations effect the form of Eqs. (9) and (10). Bartelt and Evans[23] studied the island-island correlations for approximate models of irreversible growth. Talbot and Willis[31] investigated the effect of these correlations on the "sink strength" (or capture number) of voids in irradiated material. In the interest of calculating the correct distribution function (verified with KMC simulations), a similar analysis is warranted for the current problem.

ACKNOWLEDGMENTS

We thank A. Zangwill for useful discussions and a critical reading of the manuscript. We also thank D.D. Johnson and J.L. Stevens for a critical reading of the manuscript. Support for this work has been provided by the U.S. Department of Energy, Office of Basic Energy Sciences, Division of Materials Sciences under Contract No. DE-AC04-94AL85000.

[1] R.Q. Hwang, J. Schröder, C. Günther, and R.J. Behm, Phys. Rev. Lett. **67**, 3279 (1991); C. Günther, S. Günther, R.Q. Hwang, J. Schröder, J. Vrijmoeth, and R.J. Behm, Ber. Bunsenges. Phys. Chem. **97**, 522 (1993); R.Q. Hwang, C. Günther, J. Schröder, S. Günther, E. Kopatzki, and R.J. Behm, J. Vac. Sci. Technol. A **10**, 1970 (1992).

[2] E. Bauer and W. Telieps, in *Surface and Interface Characterization by Electron and Optical Methods*, edited by A. Howie and U. Valdie (Plenum, New York, 1988), p. 195.

[3] M.A. Von Hove, W.H. Weinberg, and C.-M. Chen, *Low Energy Electron Diffraction* (Springer, Berlin, 1986).

[4] P.H. Fuoss, D.W. Kisker, G. Renaud, K.L. Tokuda, S. Brennan, and J.L. Kahn, Phys. Rev. Lett. **63**, 2389 (1989).

[5] T.A. Witten and L.M. Sander, Phys. Rev. Lett. **47**, 1400 (1981); Phys. Rev. B **27**, 5686 (1983).

[6] M. Bott, T. Michely, and G. Comsa, Surf. Sci. **272**, 161 (1992).

[7] M. Avignon and B.K. Chakraverty, Proc. R. Soc. London, Ser. A **310**, 277 (1969).

[8] G.S. Bales and A. Zangwill, Phys. Rev. B **41**, 5500 (1990).

[9] R. Kunkel, B. Poelsema, L.K. Verheij, and G. Comsa, Phys. Rev. Lett. **65**, 733 (1990).

[10] Y.W. Mo, J. Kleiner, M.B. Webb, and M.B. Lagally, Phys. Rev. Lett. **66**, 1998 (1991).

[11] S. Stoyanov and D. Kashchiev, in *Current Topics in Materials Science*, edited by E. Kaldis (North-Holland, Amsterdam, 1981), Vol. 7, pp. 69–141.

[12] J. Villain, A. Pimpinelli, and D.E. Wolf, Comments Cond. Mater. Phys. **16**, 1 (1992); J. Villain, A. Pimpinelli, L. Tang, and D.E. Wolf, J. Phys. (Paris) I **2**, 2107 (1992).

[13] J.A. Venables, Philos. Mag. **27**, 697 (1973); J.A. Venables, G.D.T. Spiller, and M. Hanbücken, Rep. Prog. Phys. **47**, 399 (1984).

[14] H.C. Kang and W.H. Weinberg, J. Chem. Phys. **90**, 2824 (1989).

[15] P.A. Maksym, Semicond. Sci. Technol. **3**, 594 (1988).

[16] L. Tang, J. Phys. (Paris) I **3**, 935 (1993).

[17] M.C. Bartelt and J.W. Evans, Surf. Sci. **298**, 421 (1993).

[18] J.G. Amar, F. Family, and P. Lam, in *Mechanisms of Thin Film Evolution*, edited by S.M. Yalisove, C.V. Thompson, D.J. Eaglesham, MRS Symposia Proceedings No. 317 (Materials Research Society, Pittsburgh, 1994).

[19] B. Lewis, Surf. Sci. **21**, 273 (1970).

[20] M. Kardar, G. Parisi, and Y.C. Zhang, Phys. Rev. Lett. **56**, 889 (1986).

[21] P. Meakin, Rep. Prog. Phys. **55**, 157 (1992); T. Vicsek, *Fractal Growth Phenomena* (World Scientific, Singapore, 1989).

[22] D. Stauffer and A. Aharony, *Introduction to Percolation Theory* (Taylor & Francis, London, 1992)

[23] M.C. Bartelt and J.W. Evans, Phys. Rev. B **46**, 12675 (1992).

[24] J.A. Blackman and A. Wilding, Europhys. Lett. **16**, 115 (1991).

[25] C. Ratsch, A. Zangwill, P. Šmilauer, and D.D. Vvedensky, Phys. Rev. Lett. **72**, 3194 (1994).

[26] D.D. Vvedensky, A. Zangwill, C.N. Luse, and M.R. Wilby, Phys. Rev. E **48**, 852 (1993).
[27] S. Clarke and D.D. Vvedensky, J. Appl. Phys. **63**, 2272 (1988); D.D. Vvedensky, S. Clarke, K.J. Hugill, A.K. Myers–Beaghton, and M.R. Wilby, in *Kinetics of Ordering and Growth at Surfaces*, edited by M.G. Lagally (Plenum, New York, 1990), Vol. B239, pp. 297–312.
[28] P. Šmilauer, M.R. Wilby, and D.D. Vvedensky, Phys. Rev. B **47**, 4119 (1993).
[29] Z.-J. Tian and T.S. Rahman, Phys. Rev. B **47**, 9751 (1993).
[30] I.M. Lifshitz and V.V. Slyozov, J. Phys. Chem. Solids **19**, 35 (1961); C. Wagner, Z. Electrochem. **65**, 581 (1961).
[31] D.R.S. Talbot and J.R. Willis, Proc. R. Soc. London, Ser. A **370**, 351 (1980).
[32] J.H. Yao, K.R. Elder, H. Guo, and M. Grant, Phys. Rev. B **45**, 8173 (1992).
[33] By writing Eq. (11) the nonlinearity, which results from a direct spatial coarse graining of Eq. (10) is avoided (see Ref. 34). A similar form can be obtained by expanding $n_1(r,\theta)$ around its average value and neglecting higher-order (nonlinear) terms.
[34] A.K. Myers-Beaghton and D.D. Vvedensky, Phys. Rev. B **42**, 5544 (1990).
[35] The rate equations calculate the density of monomers on the bare substrate. The adatoms that land on top of the islands are accounted for by the direct capture terms. Hence, to compare KMC to the rate equations, only the monomers on the bare substrate should be counted.
[36] H.G.E. Hentschel and F. Family, Phys. Rev. Lett. **66**, 1982 (1991).
[37] R.R. Kariotis and M.G. Lagally, Surf. Sci. **216**, 557 (1989); C.E. Aumann, R. Kariotis, and M.G. Lagally, J. Vac. Sci. Technol. A **7**, 2180 (1989); R. Kariotis and M.G. Lagally, J. Vac. Sci. Technol. B **7**, 269 (1989).

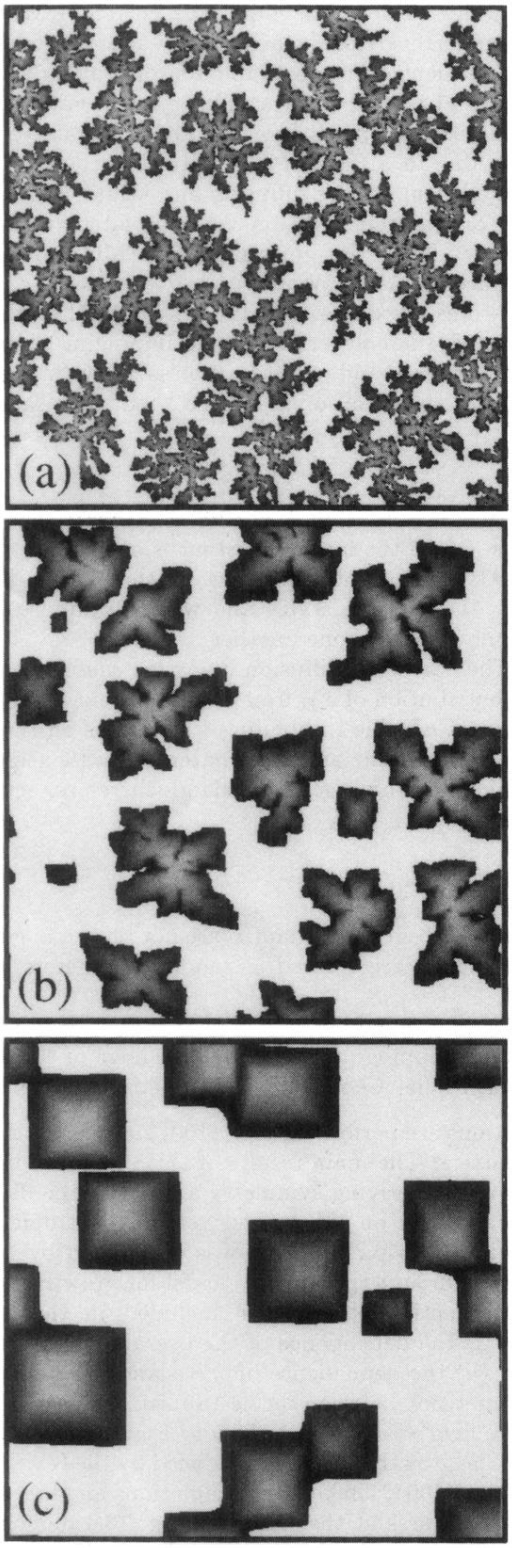

FIG. 1. Kinetic Monte Carlo simulations of irreversible island growth at three different temperatures: (a) $T = E_D/16$, $\frac{D}{F} \simeq 1 \times 10^{10}$; (b) $T = E_D/14$, $\frac{D}{F} \simeq 8 \times 10^{10}$; and (c) $T = E_D/10$, $\frac{D}{F} \simeq 4 \times 10^{12}$. The barrier to edge diffusion $E = E_D$. The lighter shades of gray represent atoms deposited at early times, while the darker shades represent those deposited at later times.